Preprints of the 18th IFAC World Congress
Milano (Italy) August 28 - September 2, 2011

Excitation control for improving transient stability limit and voltage regulation with dynamic loads

M. J. Hossain[*], **H. R. Pota**[*], **M. A. Mahmud** [*], **R. A. Ramos** [**] ,

[*] *SEIT, UNSW@ADFA, Canberra, ACT-2600, Australia.*
e-mail: (m.hossain, h-pota)@adfa.edu.au
[**] *Dept. of Electrical Engg., Engineering School of São Carlos, Brazil.*
e-mail: ramos@sc.usp.br

Abstract: This paper presents a new robust control methodology to improve the power system transient stability and voltage regulation in interconnected power systems including dynamic loads. The inclusion of dynamic load model significantly increases the nonlinearity of the system. The automatic voltage regulation (AVR) and power system stabiliser (PSS) design problems are coordinated for the augmentation of stability. The nonlinear behaviour of power systems has been represented in this paper by an uncertain term, derived from the Cauchy remainder of the Taylor series expansion. An IEEE benchmark test system has been used to demonstrate the performance of the designed controller. Large disturbance simulations demonstrate that the proposed controller enhances voltage stability as well as transient stability of a power system during severe transients.

1. INTRODUCTION

In modern power systems, improved transient and dynamic voltage stability are very important considerations to provide reliable and efficient operation of the transmission system. The use of PSSs has become increasingly important to provide improved stabilisation of the system. The PSS has been designed to add damping to the generator rotor oscillations; however, the voltage modes cannot be stabilised using a PSS; see Hossain et al. [2010b]. Generators equipped with a PSS and an AVR can enhance voltage as well as transient stability of power systems. North American Reliability Council and Western Electric Coordinating Council are ruling that machines rated more than 35 MVA or group of machines equal to or more than 75 MVA connected to the transmission grid through one transformer must operate in voltage regulating mode and be equipped with power system stabiliser to improve the transient stability of the system; see Schaefer and Kim [2006].

Power oscillations of small magnitude and low frequency often persist for long periods of time. In some cases, this presented a limitation on the amount of power able to be transmitted within the system. Recently the problem in voltage instability also is likely to increase because of the growing use of dynamic motor loads for air conditioning, heat pumps, refrigeration, etc.; see Leon and Taylor [2002]. The disturbances in power systems may not only cause the system losing synchronism but also result in short-term voltage dips and sags. This requires the control system to have the ability to suppress the potential instability due to poorly damped power angle oscillations that can be dangerous for the system stability, and to compensate the voltage dips and sags that can damage both utility and customer equipments. To improve overall system performance, the coordination between PSSs and AVR controllers have been reported in the literature; see e.g., Bevrani and Hiyama [2006, 2007], Lawt et al. [August 1994], Saidy [1997]. Some of these methods are based on the complex nonlinear simulation and the others are based on the linearised power system model.

Although the existing classical controllers have good dynamical performance for a wide range of operating conditions and disturbances, however, the real electric power system have been experiencing a dramatic change in recent years. Because of that, a great deal of attention has been paid to the application of advanced control techniques in power systems as one of the most promising application areas; see Bevrani and Hiyama [2006]. A coordinated AVR and PSS control has been presented for a single machine infinite bus system (SIMB) which allows coordinated trade-off of voltage regulation and damping enhancements; see Lawt et al. [August 1994]. A robust linear controller has been proposed to solve the problem of coordinating the control of the generator terminal voltage and electric power variations; see Heniche et al. [1995]. A unified approach for voltage regulator and power system stabiliser design based on predictive control in the *s*-domain is presented; see Saidy [1997].

Although power systems have a highly nonlinear behaviour, most of the existing excitation controllers are designed by classical control techniques in the frequency domain, involving linearisation around a nominal operating point. The controller is then designed for the linearised nominal model and a posteriori verification of controller performance is performed with the closed loop nonlinear model of the system under various operating conditions. However, this controller cannot stabilise the system for severe large disturbances. This motivates the use of advanced control techniques that consider the nonlinear interactions and ensure stability for large disturbances.

Since the transient stability and voltage regulation are ascribed to different causes, some recent proposed scenarios apply a switching strategy of two different kinds of controller to cover the different behaviour of system operation during transient period and post-transient period; see Guo et al. [November 2001], Yadaiah et al. [2004]. The performance of these schemes essentially depends upon the selection of switching time. Moreover, using different control surfaces through a highly nonlinear structure increases the complexity of the designed controllers.

The inclusion of dynamic loads provides a better representation of the actual power systems in general, but that representation exhibits even more nonlinear behaviours than the ones with constant impedance loads do. Therefore, the need for a controller that can deal with these more complex nonlinearities stems from a better representation of the actual power system behaviour.

In this paper, we consider the problem of designing a linear controller for a nonlinear power system model, in such a way that this linear controller provides an acceptable performance over a wider operating region, as compared to other conventional linear controllers. The nonlinearities are dealt with by explicitly including the information about the system nonlinearities in the design formulation, using the Cauchy remainder of the Taylor series expansion; see Hossain et al. [2010a], Hossain et al. [2009]. The voltage controller and PSS are designed sequentially provided that the performance of one controller is not degraded by the other controller. The designed controllers improve both the damping of electromechanical oscillations and voltage stability.

The organisation of the paper is as follows: Section 2 provides the mathematical modelling of the power system devices under consideration, and test system and control task are presented in Section 3. Section 4 describes the linearisation technique and the process for obtaining the bounds on the nonlinear terms. Controller design algorithm and performance of the controller are outlined in Section 5. Section 6 draws the conclusion.

2. POWER SYSTEM MODEL

Under typical assumptions, the synchronous generator can be modelled by the following set of nonlinear differential equations; see Hossain et al. [2008]:

$$\dot{\delta} = \omega\omega_s - \omega_s, \tag{1}$$

$$\dot{\omega} = \frac{1}{2H}\left[P_m - E'_q I_q - D\omega\right], \tag{2}$$

$$\dot{E}'_q = \frac{1}{T'_{d0}}\left[E_{\rm fd} - E'_q - (X_d - X'_d)I_d\right], \tag{3}$$

where $E_{\rm fd}$ is the equivalent emf in the exciter coil, δ is the power angle of the generator, ω is the rotor speed with respect to a synchronous reference, E'_q is the transient emf due to field flux linkage, ω_s is the absolute value of the synchronous speed in radians per second, H is the inertia constant of the generator, D is the damping constant of the generator, T'_{do} is the direct-axis open-circuit transient time constant of the generator, X_d is the synchronous reactance, X'_d is the transient reactance, I_d and I_q are direct and quadrature axis components of stator current, respectively. The mechanical input power P_m to the generator is assumed to be constant.

The excitation system is a high gain static system and terminal voltage is measured using a transducer with first-order dynamics:

$$E_{\rm fd} = K_a(V_c + V_{pss}),\ \dot{V}_{tr} = \frac{1}{T_r}\left[-V_{tr} + V_t\right], \tag{4}$$

where V_{tr} and T_r are the output and time constant of the voltage transducer, K_a is the gain of the exciter amplifier, $V_t = [(E'_q - X'_d I_d)^2 + (X'_d I_q)^2]^{\frac{1}{2}}$, is the generator terminal voltage and V_c is the input to the exciter (output of the designed controller).

The output-feedback controller, shown in Fig. 1, is represented as:

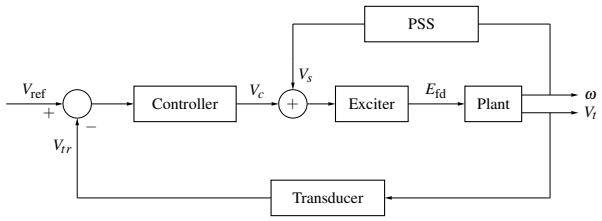

Fig. 1. Excitation Controller

$$\dot{\hat{x}}_c = A_c\hat{x}_c(t) + B_c(V_{ref} - V_{tr}), \quad V_c = C_c\hat{x}_c(t),$$

where A_c, B_c and C_c are the appropriate matrices of the controller.

A third-order model for induction motor is used in this paper; see Hossain et al. [2010b]. However, these equations represent the induction machine in its own direct and quadrature axes, which are different from the d- and q- axes of the generator. A transformation is used to represent both dynamic elements with respect to the same reference frame; see Hossain et al. [2010b]. Then, the modified third-order induction machine model can be rewritten as:

$$(V_d + jV_q) = -(R_s + jX')(I_{dm} + jI_{qm}) + jE'_{qm}, \tag{5}$$

$$\dot{s} = \frac{1}{2H_m}\left[T_m - E'_m I_{qm}\right], \tag{6}$$

$$\dot{E}'_m = -\frac{1}{T'_{dom}}\left[E'_m + (X - X')I_{dm}\right], \tag{7}$$

$$\dot{\delta}_m = s\omega_s - \omega_s - \frac{X - X'}{T'_{dom}E'_m}I_{qm}. \tag{8}$$

The block diagram of the proposed controller is given in Fig. 1. Speed and the terminal voltage of generator are used as the feedback signals. In this paper, a coordinated PSS and voltage stability controller will be designed as suggested by the auxiliary input V_s in Fig. 1.

3. TEST SYSTEM AND CONTROL TASK

One-line diagram of the 10 Machine New England system is shown in Fig 2. This system has been modified by adding a large induction motor at the terminal of each generator and the modified system is used as a test system in this paper. Generator 1 represents the aggregation of a large number of generators. The generation, and total load in this system are 6193.41 MW and 6150.5 MW respectively. The load in this paper is modelled as (i) 50% induction motor load, (ii) 5% transformer exciting current, (iii) 10% constant power, and (iv) 35% constant impedance load.

The test system in this paper, with 50% dynamic load, has one unstable mode with a real eigenvalue at 0.45 and an undamped mode with eigenvalue of $-0.0091 \pm j3.1$. Most significant normalized participation vectors for these two modes are shown in Table 1. The mode $-0.0091 \pm j3.1$ is an electromechanical mode with a damping ratio of 0.0029. The other mode with the eigenvalue 0.45 is a monotonic mode associated with the rotor electrical dynamics of generators and induction motor. This monotonic mode is introduced due to the replacement of constant impedance loads with induction motors. In this paper, attention is directed to the design of robust control for these critical modes.

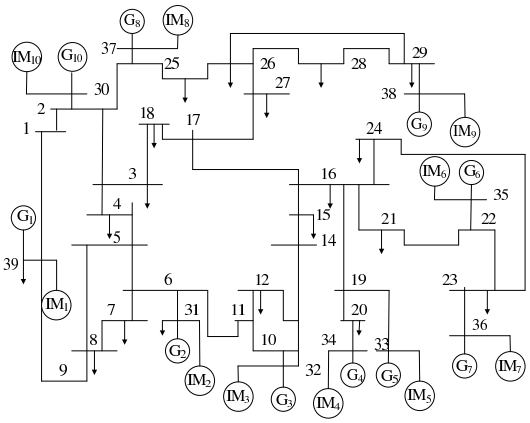

Fig. 2. Test System.

Table 1. Critical Modes and Participation factors

Modes	Participation factors		
$-0.0091 \pm j3.1$	$\triangle\omega_2 = 1$	$\triangle\delta_2 = 0.99$	$\triangle\omega_3 = 0.26$
0.45	$\triangle E'_{q4} = 1$	$\triangle E'_{qr_4} = 0.78$	$\triangle E'_{dr_4} = 0.71$

The objective in the PSS design is to increase damping of the electromechanical mode by adding an auxiliary signal to the AVR. PSSs are designed to have very low gains in the frequency range outside of a narrow band centred around the resonant mode frequency. This necessitates the design of controllers to maintain system stability for other unstable or lightly damped modes. In this paper PSS is designed for G_2 and AVR for G_4 using locally measured signal.

4. LINEARISATION AND UNCERTAINTY MODELING

Conventionally, a linear controller is designed by neglecting the higher order terms of the Taylor series around an equilibrium point. In this paper, we propose the use of a linearisation scheme which retains the contributions of the higher order terms in the form of the Cauchy remainder.

The reformulation proposed in this paper using Cauchy remainder allow us to represent the nonlinear power system models as:

$$\triangle\dot{x}(t) = A\triangle x(t) + B_1\triangle u(t) + B_2\xi(t), \tag{9}$$

$$y(t) = C_2\triangle x(t) + D_2\xi(t)), \tag{10}$$

$$\zeta(t) = C_1\triangle x(t), \tag{11}$$

where $\triangle x$ is the state vector, $\triangle u$ is the control input, $y(t)$ is the measured output, ξ is known as the uncertainty input, and ζ is known as the uncertainty output. The procedure for obtaining the matrices in (9)–(11) and bounding uncertainty has been described in the rest of this section.

Let (x_0, u_0) be an arbitrary point in the control space; using the mean-value theorem, the test system dynamics can be rewritten as follows:

$$\dot{x} = f(x_0,u_0) + L(x-x_0) + M(u-u_0), \tag{12}$$

where

$$L = \left[\left.\frac{\partial f_1}{\partial x}\right|_{\substack{x=x^{*1}\\u=u*1}}, \ldots, \left.\frac{\partial f_8}{\partial x}\right|_{\substack{x=x^{*8}\\u=u*8}}\right]^T,$$

$$M = \left[\left.\frac{\partial f_1}{\partial u}\right|_{\substack{x=x^{*1}\\u=u*1}}, \ldots, \left.\frac{\partial f_8}{\partial u}\right|_{\substack{x=x^{*8}\\u=u*8}}\right]^T, \quad f = [f_1, \ldots, f_8]^T,$$

where (x^{*p}, u^{*p}), $p = 1, \cdots, 7$, denote points lying in the line segment connecting (x,u) and (x_0,u_0) and f denotes the vector function on the right-hand side of the vector differential equations.

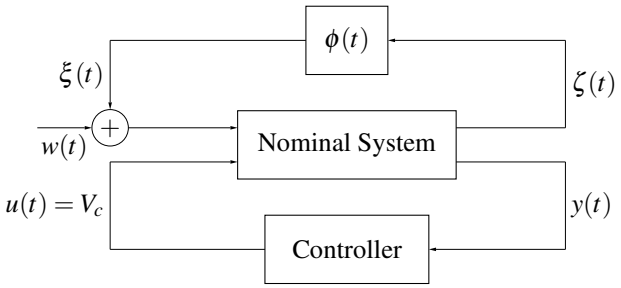

Fig. 3. Voltage control scheme

Letting (x_0,u_0) be the equilibrium point and defining $\Delta x \triangleq x - x_0$ and $\Delta u \triangleq u - u_0$, it is possible to rewrite (12) as follows

$$\begin{aligned}\Delta\dot{x} &= \dot{x} - \dot{x_0},\\ &= A\triangle x + (L-A)\triangle x + (M-B_1)\triangle u + B_1\triangle u,\end{aligned} \tag{13}$$

where $A = \left.\frac{\partial f}{\partial x}\right|_{\substack{x=x_0\\u=u_0}}$, $B_1 = \left.\frac{\partial f}{\partial u}\right|_{\substack{x=x_0\\u=u_0}}$. Equation (13) is linear with respect to the control vector. Since $x^{*p}, p = 1,\ldots,7$ are not known, it is difficult to obtain the exact value of $(L-A)$, but it is possible to obtain a bound on $\|(L-A)\|$.

The system (13) is of the form which allows for an application of the minimax control design technique; see Ugrinovskii and Petersen [2001]. To apply this technique, we rewrite system (13) in terms of the block diagram shown in Fig. 3.

In this figure, we introduce a fictitious signal ξ such that

$$(L-A)\triangle x = B_2\xi(t), \tag{14}$$

where

$$\begin{aligned}B_2 = \text{diag}\Bigg(0, \frac{X_d - X'_d}{T'_{do}}, \frac{1}{2H}, \frac{1}{T_r},\\ \frac{X_s - X'_s}{T'_{dom}}, \frac{1}{2H_m}, \frac{X_s - X'_s}{T'_{dom}}\Bigg).\end{aligned} \tag{15}$$

and

$$\xi = \tilde{\phi}(t)\tilde{C}_1\triangle x. \tag{16}$$

Matrix $\tilde{C}_1$ is chosen such that

$$\tilde{C}_1 = \begin{bmatrix} 0&0&1&0&0&0&0\\ 0&0&0&0&1&0&0\\ 0&0&0&0&0&1&0\\ 0&0&0&0&0&0&1\end{bmatrix},$$

$$(L-A)\triangle x = B_2\tilde{\phi}(t)\tilde{C}_1\triangle x \tag{17}$$

The expressions for obtaining $\tilde{\phi}(t)$ can be determined in the same way as in Hossain et al. [2010a]. The system can now be written as

$$\triangle\dot{x} = A\triangle x + B_1\triangle u + B_2\xi(t). \tag{18}$$

In general, $x^{*p}, p = 1,\ldots,7$, are not known beforehand, it is difficult to obtain the exact value of $(L-A)$, but it is possible to obtain a bound on $\phi(t)$ shown in Fig. 3.

Next we introduce a scaling parameter α and write $C_1 = \sqrt{\alpha}\tilde{C}_1$, where α scales the magnitude of the uncertain output

$$\zeta = \sqrt{\alpha}\left(\tilde{C}_1\triangle x\right). \tag{19}$$

We write $\phi(t) = \frac{1}{\sqrt{\alpha}}\left[\tilde{\phi}(t)\right]$. The value of α is chosen such that the uncertainty, $\phi(t)$, shown in Fig. 3 satisfies,

$$\|\phi(t)\|^2 \leq 1. \tag{20}$$

From this, we have

$$\|\xi(t)\|^2 \leq \alpha \|\left(\tilde{C}_1 \triangle x\right)\|^2. \quad (21)$$

and we recover the norm bound constraints Ugrinovskii and Petersen [2001],

$$\|\xi(t)\|^2 \leq \|\zeta(t)\|^2. \quad (22)$$

Condition (22) will enable us to apply the minimax LQG control design methodology to obtain a controller for the underlying nonlinear system. Robustness properties of the minimax LQG controller ensure that this controller stabilises the nonlinear system (9)–(11) for all instances of linearisation errors.

The output matrices for the voltage controller is defined as $C_2 = [0,0,0,1,0,0,0,]^T$. The theory requires that $D_2 D_2' > 0$; see Ugrinovskii and Petersen [2001]. This property is required by the design procedure but it does not represent any physical characteristics of the system, so we choose the value of D_2 as small as possible. Equations (9)–(11) provide a new representation of the power system model which contains the linear part, and also another part with higher order terms. The new formulation presented in this section is used with the minimax LQG control theory to design the excitation controllers for the generator; see et. al. Hossain et al. [2010b], Ugrinovskii and Petersen [2001] .

5. CONTROLLER DESIGN AND PERFORMANCE EVALUATION

Prior to the controller design, we carry out several large disturbance simulations to get an idea of the region of interest. The maximum value of $\phi(t)$ is obtained over this region and not globally. If the maximum value of $\phi(t)$ is evaluated over the entire uncertainty region, the calculation burden will be very high and it will lead to a conservative controller. The controller is then designed as follows:

Step 1 From the simulations of the faulted system, obtain the range of the variation of all state variable and form a polytope Ω with corner points given by $(x_{0_p} - x_{f_p})$ and $(x_{f_p} + x_{0_p})$, $p = 1, \ldots, 7$, where x_{f_p} is the largest variation of the p^{th} state variable about its equilibrium value x_{0_p}. Formally $x \in \Omega$ if $|x - x_{0_p}| \leq |x_{f_p} - x_{0_p}|$.

Step 2 Obtain

$$\alpha^* = \max_{x^{*p} \in \Omega} \left\{\alpha : ||\phi(t)||^2 < 1\right\}.$$

The process to obtain α^* involves obtaining the maximum value of $||\tilde{\phi}(t)||$ over the polytope Ω.

Step 3 Check if there exists a feasible controller with $\alpha = \alpha^*$.

Step 4 If we obtain a feasible controller in the above step, either enlarge the polytope Ω, i.e., increase the operating region of the controller, or if we have arrived at the largest possible polytope then perform an optimal search over the scalar parameter τ to get the infimum of cost function Hossain et al. [2010b]. If there is no feasible solution with the chosen $\alpha = \alpha^*$, reduce the polytope, Ω and go to Step 2.

For the given power system model, we are able to obtain a feasible controller with the value of $\alpha = 0.925$. The controller is stabilising for all variations of states in the polytope region, Ω formed by corner points $\left[\bar{\delta}, \bar{\omega}, \bar{E}_q', \bar{V}_{tr}, \bar{\delta}_m, \bar{s}, \bar{E}_m'\right]$ and $\left[\underline{\delta}, \underline{\omega}, \underline{E}_q', \underline{V}_{tr}, \underline{\delta}_m, \underline{s}, \underline{E}_m'\right]$ with the values: $|\bar{\delta} + \delta_0| = 45^\circ$, $|\underline{\delta} - \delta_0| = 45^\circ$ $|\bar{\omega} + \omega_0| = 0.375$ pu, $|\underline{\omega} - \omega_0| = 0.375$ pu, $|\bar{E'}_q + E'_{q_0}| = 0.435$, $|\underline{E'}_q - E'_{q_0}| = 0.435$, $\bar{V}_{tr} = V_{tr0} + 0.275$ pu, $\underline{V}_{tr} = V_{tr0} - 0.275$ pu, $\bar{\delta}_m = \delta_{m0} + 41.19^\circ$, $\underline{\delta}_m = \delta_{m0} - 41.19^\circ$,

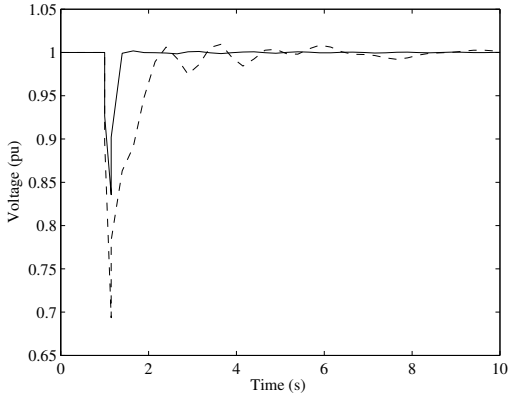

Fig. 5. Terminal Voltage (G_4) for the three-phase fault on bus 2–3. (Solid line voltage controller+PSS and dashed line voltage controller only).

$\bar{s} = s_0 + 0.225$ pu, $\underline{s} = s_0 - 0.225$ pu, $\bar{E}_m' = E_{m0} + 0.25$ pu and $\underline{E}_m' = E_{m0} - 0.25$ pu. Although the designed controller is not globally stabilising, we can be confident that it will stabilise the system for most contingencies.

In this paper PSS, shown in Fig. 4 has been designed using the standard technique which uses the change in speed $\Delta\omega$ as the feedback variable. PSS was designed subsequent to the design of voltage controller. The PSS parameters are $T_w = 5$, $K_{STAB} = 0.43$, $T_1 = 0.25$, $T_2 = 0.02$, $T_3 = 0.0.252$, and $T_4 = 0.039$.

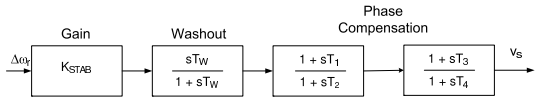

Fig. 4. PSS block diagram.

5.1 Controller performance evaluation

As mentioned earlier, the voltage controller and PSS have been designed sequentially. At first, voltage controller is designed and then the PSS is designed including voltage controller. The objective of PSS design is to damp electromechanical oscillations in power systems. However, this should not be done at the expense of reducing the voltage regulation ability of the excitation system. Using simulation results given below, we show that the PSS does not have an adverse effect on the voltage controller.

A simulation is carried out by applying a symmetrical three phase to ground short circuit fault on line 16–19. The fault is cleared after 150 ms. Figs. 5 and 6 show the terminal voltage and real power output of generator G_4 with both voltage controller plus PSS and only the voltage controller. Fig. 5 shows that the PSS improves the voltage response. This is due to the improved damping of the electromechanical modes, which is also visible from Fig. 6.

Responses of terminal voltage and reactive power output of generator G_2, when a two-line to ground fault (2LG) occurs on line 5–6 from phase–B and phase–C to ground, are shown in Figs. 7 and 8 respectively. From Figs. 7 and 8, it can be seen that the performance of the voltage controller is not much affected by the PSS in stabilising the voltage and producing reactive power output of generator. From these figures, it is

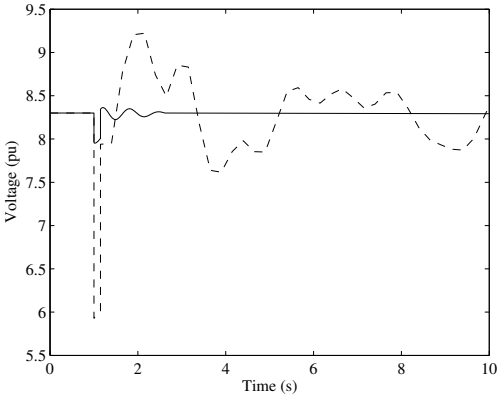

Fig. 6. Real power output (G_4) for the three-phase fault on bus 2–3. (Solid line voltage controller+PSS and dashed line voltage controller only).

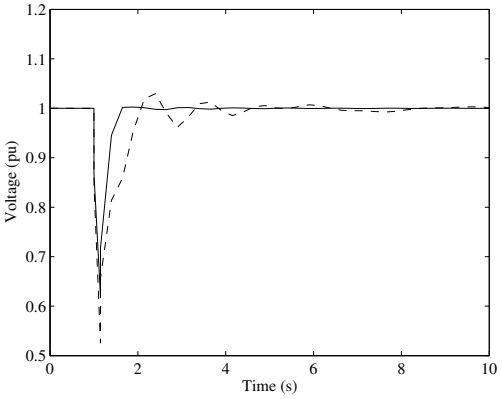

Fig. 7. Terminal Voltage (G_2) for the unsymmetrical fault on bus 5–6. (Solid line voltage controller+PSS and dashed line voltage controller only).

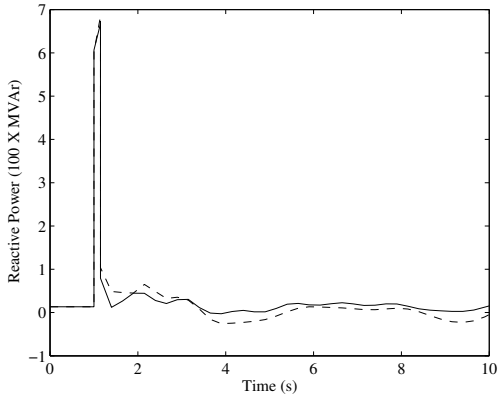

Fig. 8. Reactive power output (G_2) for the the unsymmetrical fault on bus 5–6. (Solid line voltage controller+PSS and dashed line voltage controller only).

clear that the designed controllers also stabilise the generators under unsymmetrical faults.

In the preceding part of the paper the voltage controller is designed first and then the PSS—Design A. This order of the controller design is compared with the design where the

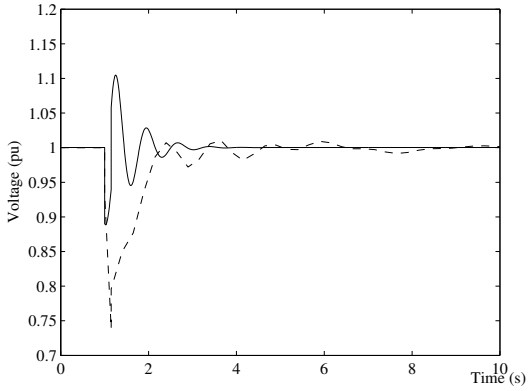

Fig. 9. Terminal Voltage (G_4) for 20% change in load at bus 20. ((Solid line controllers with Design A and dashed line Design B).

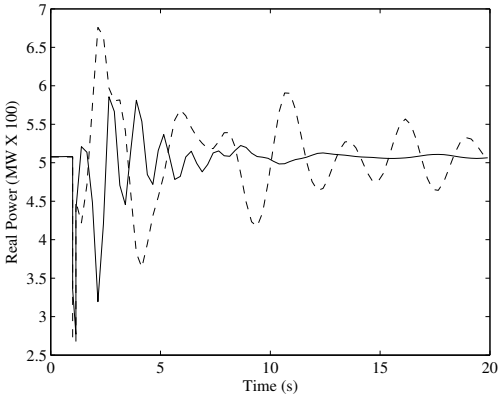

Fig. 10. Real power output (G_4) for 20% change in load at bus 20. (Solid line controllers with Design A and dashed line Design B).

PSS is designed first and then the voltage controller—Design B. The closed-loop dominant modes are, Design A: $-0.51 \pm j0.326$ and with Design B: $-0.0091 \pm j3.04$. The closed-loop behaviour is also compared for a 20% increase in load at bus 20. The terminal voltage and real power at generator G_4 is shown in Figs. 9 and 10. With Design B the terminal voltage dips to approximately 0.75pu and the real power oscillates for well over 20 s with a peak of 670 MW. The response for Design A is well damped and both terminal voltage and real power stay within a narrow and acceptable range. This result can be explained by the fact that in Design B, the voltage controller changes the required phase lead to be provided by the PSS.

The performance of the designed controllers are also compared with the performance of the conventional IEEE AC1A exciter and IEEEST stabiliser. Here, a simulation is performed for a severe symmetrical three-phase fault at bus 20. The fault is cleared after 0.15s. Figs. 11 and 12 show terminal voltage and angle response of the generator G_4 and G_2, respectively. From Figs. 11 and 12, we can see that the proposed controller stabilises voltage within few cycles of fault occurrence and damps out the power angle oscillations. It is clear that the proposed controller has a better performance in terms of settling time, damping, overshoot and oscillations.

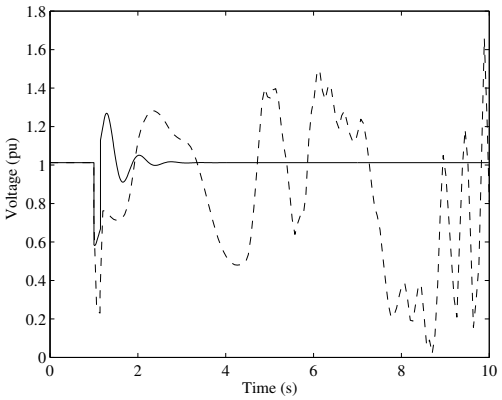

Fig. 11. Terminal Voltage (G_4) for the three-phase fault. (Solid line designed controllers and dashed line AC1A exciter and IEEEST stabiliser).

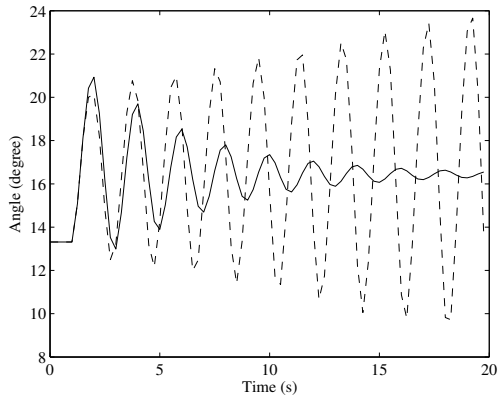

Fig. 12. Angle response (G_2) for the three-phase fault. (Solid line designed controllers and dashed line AC1A exciter and IEEEST stabiliser).

6. CONCLUSIONS

In this paper an algorithm to design robust output feedback excitation controllers is proposed. Detailed modeling of each component and a suitable control strategy of excitation system are presented. The problem of damping electromechanical oscillation and improving voltage stability have been addressed and taken into account in the overall proposed controller. With the proposed reformulation, it becomes easier to explicitly account for the effect of nonlinearities in the system dynamics, which enables us to more accurately represent the system and also provides guaranteed performance and stability characteristics over a pre-specified region around the equilibrium point, when compared conventional linearisation procedure. The resulting controller is practically realisable and valid within a wide range of operating conditions. Simulation results show that the proposed control scheme works well in accordance with the standard PSS and can improve dynamic performance of the multi-machine power system effectively. Our proposed treatment of the nonlinearities is an advance with respect to the current practice because it deals in a rigorous and efficient manner with the nonlinear behaviours induced by the dynamic loads.

REFERENCES

H. Bevrani and T. Hiyama. Stability and voltage regulation enhancement using an optimal gain vector. In *IEEE Power Engineering Society General Meeting*, pages 1–6, Canada, 2006.

Hassan Bevrani and Takashi Hiyama. Robust coordinated AVR-PSS design using H_∞ static output feedback control. *IEEJ Trans. on Power and Energy*, 127(1):70–76, 2007.

Y. Guo, D. J. Hill, and Y. Wang. Global transient stability and voltage regulation for power systems. *IEEE Trans. on Power Systems*, 16(4):678–688, November 2001.

A. Heniche, H. Bourles, and M. P. Houry. A desensitized controller for voltage regulation of power systems. *IEEE Trans. on Power Systems*, 10(3):1461–1465, 1995.

M. J. Hossain, H. R. Pota, and V. Ugrinovski. Short and long-term dynamic voltage instability. In *17th IFAC World Congress*, pages 9392–9397, Seoul, Korea, July 6-11 2008.

M. J. Hossain, H. R. Pota, V. Ugrinovskii, and R. A. Ramos. A novel STATCOM control to augment LVRT capability of fixed-speed induction generators. In *48th IEEE Conference on Decision and Control*, pages 7843–7848, Shanghai, China, December 16–18 2009.

M. J. Hossain, H. R. Pota, V. Ugrinovskii, and R. A. Ramos. Simultaneous STATCOM and pitch angle controls for improved LVRT capability of fixed-speed wind turbines. *IEEE Trans. on Sustainable Energy*, 1(3):142–151, October 2010a.

M. J. Hossain, H. R. Pota, V. Ugrinovskii, and Rodrigo A. Ramos. Voltage mode stabilisation in power systems with dynamic loads. *International Journal of Electrical Power and Energy Systems*, 32(9):911–920, November 2010b.

K. T. Lawt, D. J. Hill, and N. R. Godfrey. Robust co-ordinated AVR-PSS design. *IEEE Trans. on Power Systems*, 9(3): 1218–1225, August 1994.

J. A. Diaz De Leon and C. W. Taylor. Understanding and solving short term voltage stability problems. In *IEEE Power Engineering Society Summer Meeting*, pages 745–752, Chicago, USA, July 2002.

M. Saidy. A unified approach to voltage regulator and power system stabiliser design based on predictive control in analogue form. *International Journal of Electrical Power & Energy Systems*, 19(2):103–109, 1997.

Richard C. Schaefer and Kiyong Kim. Power system stabilizer performance with summing point type var/power factor controllers. In *Conference Record of the 2006 IEEE IAS Pulp and Paper Conference*, pages 1–7, 2006.

V. A. Ugrinovskii and I. R. Petersen. Minimax LQG control of stochastic partially observed uncertain systems. *SIAM J. Control Optim.*, 40(4):1189–1226, 2001.

N. Yadaiah, A. G. D. Kumar, and J. L. Bhattacharya. Fuzzy based coordinated controller for power system stability and voltage regulation. *Electric Power Systems Research*, 69(2–3):169–177, 2004.